ENGINEERING Management 2026, 13(1): 194–212
https://doi.org/10.1007/s42524-026-5157-8

RESEARCH ARTICLE

Ying YANG, Jiahao ZHAN, Yang LIU, Xiaobo QU

Cross-city transfer learning for optimal e-scooter parking station deployment: Evidence from 25 European cities

Abstract The rapid growth of shared e-scooters has presented new challenges for urban management, especially in cities newly introducing the service, where scientifically planning parking stations to prevent disorganized parking is a time-consuming and costly problem. This paper proposes a cross-city transfer learning framework designed to rapidly predict rational layouts for fixed e-scooter parking stations in data-sparse new cities. The method utilizes operational data from 25 European cities and multi-source urban open-space data, constructing a transfer prediction model by discretizing cities into hexagonal grids and embedding spatial feature vectors. The results indicate that the effectiveness of group-based transfer learning is significantly influenced by geographic location, population size, and economic level, with the most effective transfers occurring between economically similar cities (an average F1-score of 0.801 for the super-high-income group). Additionally, our multi-dimensional city similarity matching strategy—based on socio-economic, point-of-interest (POI) distribution, and spatial structure features—demonstrates better stability and generalization, particularly in achieving the Top-3 similarity match. This research provides city planners and operators with data-driven insights to design shared e-scooter parking infrastructure efficiently.

Received Jun. 22, 2025; revised Aug. 15, 2025; accepted Sep. 8, 2025

Ying YANG, Jiahao ZHAN
School of Management, Shanghai University, Shanghai 200444, China

Yang LIU (✉), Xiaobo QU
School of Vehicle and Mobility, Tsinghua University, Beijing 100084, China; State Key Laboratory of Intelligent Green Vehicle and Mobility, Tsinghua University, Beijing 100084, China
E-mail: thu_ets_ly@tsinghua.edu.cn

This work was supported by the National Natural Science Foundation of China (Nos. 72401174, 52572334, 52221005, and 52220105001), the Independent Research Project of the State Key Laboratory of Intelligent Green Vehicle and Mobility, Tsinghua University (No. ZZ-GG-20250403), and Tsinghua University (State Key Laboratory of Intelligent Green Vehicle and Mobility)–Hangzhou Airport Economic Demonstration Zone Joint Research Center for Integrated Transportation, China.

Keywords shared e-scooter, parking planning, cross-city, transfer learning, urban similarity

1 Introduction

The shared e-scooter was first introduced in 2017, and with its flexible, convenient, and low-carbon characteristics, it has met the daily commuting and travel needs of urban residents (Cao et al., 2021; Li et al., 2022; Fuady et al., 2024; Krauss et al., 2024). This flexible and engaging mode of transportation is particularly suitable for first- and last-mile travel, making shared e-scooters a crucial part of short-distance trips and an essential connection to other forms of transport in modern cities (Guo et al., 2023; Tuli and Mitra, 2024; Vinagre Díaz et al., 2024). However, the rapid proliferation of shared e-scooters has also brought new challenges for urban management, particularly the disorganized distribution of parking stations (Brown, 2021a). Due to the high flexibility of shared e-scooters, they are often parked without restrictions at designated stations, leading to unregulated street parking (Zakhem and Smith-Colin, 2021). This behavior can result in road obstructions, damage the urban landscape, and even create traffic safety hazards (Brown et al., 2020; Klein et al., 2023). The underlying cause of these issues is partly the inadequate or poorly planned allocation of fixed e-scooter parking stations by city managers. Therefore, the introduction of e-scooters and the rise of shared micro-mobility should prompt cities to reassess how to manage these new services properly and effectively, thereby maximizing public benefits (Yang et al., 2025a).

Shared e-scooters are predominantly active in developed cities and regions in Europe and North America (Abouelela et al., 2023; Bieliński and Ważna, 2020). The setup of e-scooter parking stations in these cities is generally based on operational e-scooter distribution data, from which urban management practices are derived or static rules are established (Brown et al., 2021b; Fearnley, 2020). In other words, these cities typically build travel demand models by conducting long-term surveys of

citizens' travel patterns (Peled et al., 2021; Emami and Ramezani, 2024) and only begin deploying public facilities after gathering substantial amounts of data. However, for new cities that wish to introduce shared e-scooters, this process undoubtedly involves high design costs and extended time, making it difficult to respond quickly to the city's dynamic demand (Hurlet et al., 2024).

To address this challenge, we propose a cross-city transfer learning framework that leverages operational data from shared e-scooters in 25 established European cities, multidimensional urban characteristics, and open-source data from OpenStreetMap (OSM). The core of our methodology involves discretizing each city into hexagonal grids and constructing rich feature vectors that embed detailed Points of Interest (POI) information and account for the influence of neighboring grids. Crucially, we introduce a novel multidimensional city similarity metric to systematically evaluate the resemblance between cities based on their socio-economic characteristics, POI distributions, and spatial structures. This metric enables the selection of the most suitable source cities for knowledge transfer, thereby enhancing the accuracy of predictions. By applying machine learning models, our framework predicts the suitability of each grid in a new, data-sparse target city for hosting a fixed parking station. This approach provides urban planners with a robust, data-driven initial layout, significantly reducing the reliance on costly and time-consuming local data collection.

Our core theoretical innovation lies in developing a multi-dimensional urban similarity matching strategy that moves beyond traditional single-factor approaches, providing a robust foundation for cross-city knowledge transfer in urban infrastructure planning. The main contributions of this paper are as follows: (1) We propose a novel multi-dimensional city similarity matching strategy, which integrates socio-economic, POI distribution, and spatial structure features to identify optimal source cities for knowledge transfer. (2) We develop a practical cross-city transfer learning framework that operationalizes this strategy with advanced feature engineering, including neighborhood influence modeling, to predict e-scooter parking demand effectively. (3) We provide extensive empirical validation across 25 European cities, demonstrating that our similarity-based approach is more stable and effective than conventional grouping methods, thus offering actionable guidance for urban planning. The framework of this paper is shown in Fig. 1.

The remainder of this paper is organized as follows: Section 2 summarizes research on micro-mobility parking planning and cross-city applications; Section 3 describes the data sources and methodology; Section 4 discusses the model's predictive performance; and Section 5 is the conclusion including some policy recommendations and limitations for possible future research.

2 Literature review

Shared micro-mobility services are particularly suited for short-distance urban travel. However, the surge of e-scooters has led to street congestion and disorganized parking in cities. Irrational parking planning hinders operators' ability to deploy vehicles efficiently, leading to wasted resources and higher maintenance costs (Deveci et al., 2023). Many studies have explored the planning of parking areas for various shared micro-mobility tools in

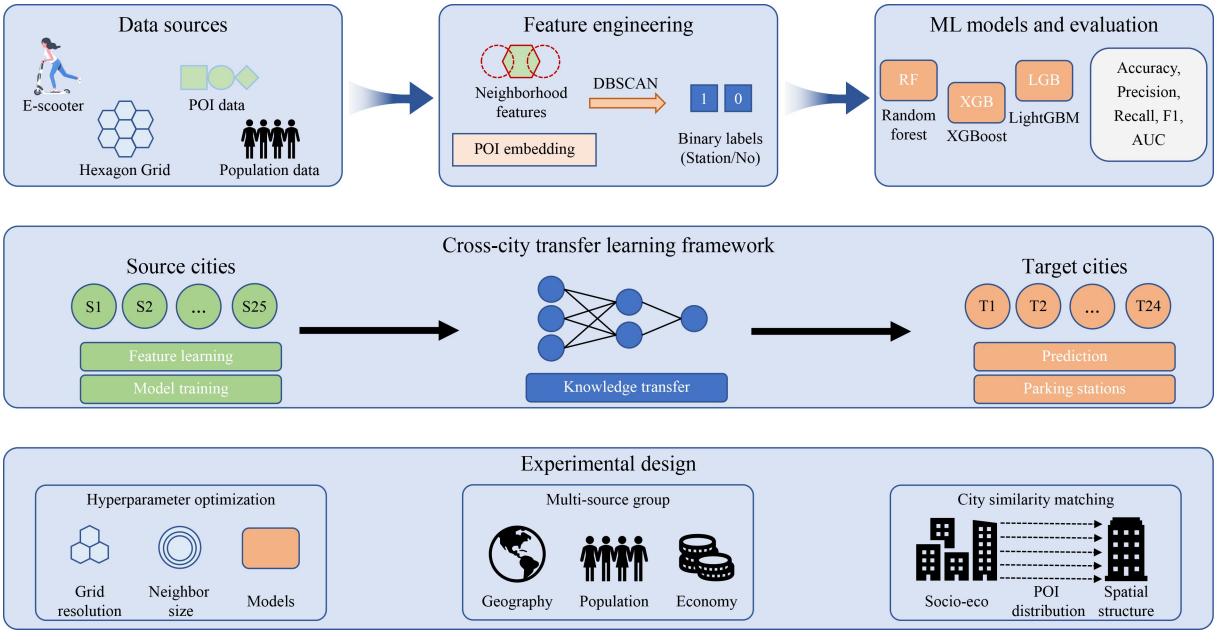

Fig. 1 Framework of cross-city e-scooter parking prediction.

urban environments. Moreover, the transfer of computational tasks across cities has been widely applied to introduce shared services in new cities.

2.1 Parking planning of shared micro-mobility

Planning shared e-scooter parking stations is a site selection or location-allocation problem for shared mobility stations (Colovic et al., 2024). Current research focuses on station planning for micro-mobility vehicles, such as shared bicycles and e-scooters (Yin et al., 2023). These planning strategies generally fall into two categories: fixed parking or charging areas and dynamic management. In fixed parking area management, governments or operating companies designate specific parking zones in the city to reduce random parking behaviors (Button et al., 2020; Gössling, 2020). These zones are typically established based on policy guidance and spatial availability, but lack dynamic responses to real-time parking demands (Almaskati et al., 2024). On the other hand, dynamic management strategies aim to adjust parking distribution based on real-time data, such as GPS location information and user demand (Pérez-Fernández and García-Palomares, 2021). While this approach somewhat improves the utilization of parking resources, it incurs higher implementation costs and requires continuous system support. Additionally, hardware applications and user travel behavior preference analysis for micro-mobility services provide a fundamental research basis for parking station prediction and deployment (Curtale and Liao, 2023; Xie and Liao, 2024; Zhang et al., 2025).

To address the complexity of shared mobility parking station setups, data-driven parking prediction models have been proposed in recent years (Sandoval et al., 2021). These models typically plan urban parking demand by analyzing historical data and spatial characteristics (Hawa et al., 2021). Yan et al. (2024) designed an intelligent parking recommendation system for micro-mobility users by analyzing users' historical travel data, travel trajectories, and parking availability. Chen et al. (2021) generated candidate bike stations by clustering large-scale shared bicycle trajectory data and constructed a weighted directed graph model based on the clustering results. They trained a graph sequence model using a gated graph neural network to predict the next cycle of bike stations dynamically. Furthermore, several studies have combined geospatial data with machine learning algorithms to predict parking station locations. Specifically, clustering algorithms like DBSCAN (Density-Based Spatial Clustering of Applications with Noise) (Zhang et al., 2019) and K-Means (K-Means Clustering Algorithm) (Ma et al., 2019) have been widely applied in clustering analysis for shared micro-mobility to identify parking hotspot areas. These methods can also be used to analyze the geographic distribution of e-scooters, uncover potential parking demand, and optimize specific areas (Heumann et al., 2021; Ziedan et al., 2023).

Some studies have combined POI data and urban functionality information to overcome data sparsity and predict shared mobility stations (Xiao and Xu, 2024). Fazio et al. (2021) integrated socioeconomic information with public transportation accessibility and POI attractiveness, proposing a priority-based strategy for selecting locations of bicycle stations. Yue et al. (2024) combined POI data with other factors, such as population density, using the analytic hierarchy process to comprehensively evaluate demand points and generate a land suitability map, which was the basis for selecting shared e-scooter station sites. These methods embed POI data into grid-based urban areas and utilize machine learning models to infer parking station locations. Researchers can more accurately predict parking demand across various regions by analyzing the density and functional classification of different types of POIs in specific areas (Shah et al., 2023).

2.2 Application of transfer learning in cross-city computing tasks

The adaptability of the aforementioned methods across different cities remains an issue to be addressed, and transfer learning techniques in cross-city predictions have become a promising direction for further exploration (Yang et al., 2025b).

As a technique that addresses data sparsity and heterogeneity, transfer learning has gained increasing attention in urban computing (Liu et al., 2021b; Raczycki and Szymański, 2021; Wang et al., 2022). Traditional machine learning methods often rely on large amounts of labeled data; however, in real-world scenarios, data collection is costly, especially when extending models across cities (Liu et al., 2023; Kuang et al., 2024). The inconsistency and incompleteness of data between different cities present critical challenges to the generalization capability of models. Transfer learning can be achieved by training data feature patterns in source cities with abundant data and transferring them to target cities with scarce data, effectively solving the issue of data sparsity in cross-city predictions (Huang et al., 2023; Ma and Xue, 2024).

Currently, urban computing tasks primarily focus on prediction, detection, and deployment (Wang et al., 2018). Similar to cross-city shared e-scooter parking site planning, many site selection studies also include deployment tasks. Guo et al. (2018) proposed a knowledge transfer framework called City Transfer to recommend chain store locations based on multi-source urban data. They collected multi-source data from four Chinese cities, including data from chain hotel enterprises, check-in data, POI data, and housing price data, and successfully implemented chain store location recommendations within the City Transfer framework. Liu et al. (2021a)

proposed a transfer learning framework called Weighted Adversarial Networks, utilizing user, store, and POI data to address the cold-start problem in store location selection for target cities. Liu et al. (2018) combined factor analysis with a Convolutional Neural Network (CNN) to transfer knowledge of bike distribution from existing cities to new cities. Factor analysis was employed to reduce the differences in feature distribution between cities and to generate latent features. At the same time, CNN captured the impact of geographical features on bike distribution, predicting the number of bikes in each grid. He and Shin (2020) analyzed real data from dockless e-scooters and proposed a spatiotemporal graph capsule neural network-based prediction model. This model predicts reconfigured e-scooter traffic distributions to determine the planning of e-scooter parking stations.

In summary, while existing studies have made significant progress in parking spot siting and layout optimization, their methods generally rely on abundant local data, which limits their applicability in new cities where data are scarce. For example, studies based on traditional clustering algorithms are effective in analyzing hotspot areas but poorly transferable across cities, making it difficult to adapt to the diversity of urban functional layouts. These shortcomings underscore the need to bridge the cross-city prediction gap through transfer learning methods. Therefore, we aim to provide a novel solution for managing shared e-scooter parking in new cities, leveraging city POI data and applying transfer learning methods to provide an initial layout for fixed e-scooter stations quickly. Our approach addresses the critical gap by developing a comprehensive framework that integrates multi-dimensional urban similarity assessment with advanced feature engineering techniques, enabling effective knowledge transfer across diverse urban contexts while maintaining prediction accuracy suitable for practical deployment.

3 Data and methods

3.1 Data collection and processing

We utilized data from 25 European cities to evaluate the transferability of fixed parking point prediction. These cities have abundant e-scooter data, and the operational areas of e-scooters are relatively concentrated, allowing for the identification of potential fixed parking stations through clustering methods. Table 1 presents the geographic distribution, population size, and economic level classification of these cities. Population data were obtained from the publicly available European city statistics provided by World Population Review (World Population Review, 2025). The 25 cities were classified into five categories by geographic region and three categories by economic level. According to population size, the cities were divided into four groups: large cities (population >1 million), medium cities (500,000–1 million), medium-to-small cities (100,000–500,000), and small cities (population < 100,000).

The classification of economic levels was based on purchasing power standards reported by Eurostat. Specifically, we categorized the 25 cities into four levels, super high (>200%), high (150-200%), medium (100-150%), and low (< 100%), based on the purchasing power standard (PPS) per city as a percentage of the EU27 average of the corresponding NUTS 3 regions (Eurostat, 2025). For cities with available data, we directly adopted the values of their NUTS 3 regions. For cities lacking direct data, such as Tampere and Stjordal, we used the average of their broader region (e.g., Pirkanmaa, Trøndelag) or respective countries as approximations. Due to such approximations, the classification results may involve a certain degree of deviation; we further analyze the potential impact of this issue on transfer learning performance in the discussion section. In addition, we focus on collecting electric scooter trip data, POI data, and population distribution data for these cities.

(1) E-scooter Data: The shared e-scooter data of all cities is sourced from Tier, the largest e-scooter provider in Europe. Using the API of Tier (Tier, 2024), we extracted shared e-scooter data from the studied cities from 15 July to 15 September 2024. Each e-scooter's location is recorded with latitude and longitude accurate to six decimal places (approximately 0.1 m of error). To account for vehicles that might be under maintenance or have been unused for extended periods, we removed any e-scooters with identical IDs and unchanged latitude and longitude values.

In the process of transfer prediction, only source cities are assumed to have e-scooter data, which is used to derive hypothetical fixed parking stations as labeled training data. This approach enables new cities to plan parking infrastructure based on experiences from established markets without requiring local operational data. We use DBSCAN (Khan et al., 2014) to cluster the latitude and longitude data of e-scooters to identify fixed parking stations in the source cities. DBSCAN is a density-based clustering method that effectively identifies clusters based on density relationships among e-scooter data points. The algorithm uses two key parameters: ε (neighborhood radius) and minPts (minimum points required to form a core point), which determine the definition of core points, boundary points, and noise points. In our implementation, we set minPts = 5 and applied post-processing to retain only clusters with at least 10 points to ensure meaningful parking station locations.

(2) POI Data: Using the Overpass API of OSM, we obtained spatial data of the studied cities, including city boundary information. Different types of OSM data may exist in the form of nodes, ways, or relations. Based on common POI types, we categorized the OSM data into 20

Table 1 City classification in this study

Geography	Country	City	Population (million)	Economic level (percentage)
Nordic	Finland	Helsinki	Large (1.35)	High (131%)
		Tampere	Med-small (0.35)	Medium (100%)
	Norway	Trondheim	Med-small (0.21)	Medium (121%)
		Stjordal	Small (0.02)	Medium (121%)
	Sweden	Boras	Med-small (0.11)	Medium (115%)
		Varberg	Small (0.03)	Low (86%)
Central	Germany	Berlin	Large (3.58)	Medium (123%)
		Hamburg	Large (1.79)	High (189%)
		Munich	Large (1.59)	Super high (332%)
		Frankfurt	Medium (0.65)	Super high (266%)
	Austria	Innsbruck	Med-small (0.14)	Medium (130%)
		Linz	Med-small (0.20)	High (160%)
	Switzerland	Basel	Medium (0.58)	Super high (357%)
		Zurich	Large (1.46)	High (186%)
Western	Netherlands	Eindhoven	Med-small (0.37)	High (165%)
		Utrecht	Medium (0.58)	High (159%)
	France	Lyon	Large (1.79)	Medium (100%)
		CASGBS	Med-small (0.33)	Medium (105%)
Southern	Spain	Madrid	Large (6.81)	Medium (120%)
	Italy	Parma	Medium (0.63)	Medium (124%)
		Bari	Med-small (0.34)	Low (74%)
Eastern	Hungary	Budapest	Large (1.78)	High (168%)
	Poland	Krakow	Medium (0.77)	Medium (124%)
		Wroclaw	Medium (0.64)	Medium (118%)
		Gdansk	Med-small (0.47)	Low (50%)

different classes, as shown in Table 2. Specifically, considering the riding characteristics of e-scooters, we paid particular attention to the categories of *Roads_bike*, *Roads_drive*, and *Roads_walk*, which are used to calculate the length of roads within an area. For other OSM objects, we calculated either the area or the point count based on their respective field information.

(3) Population Data: World Population Review provides the total population for each city. Additionally, we obtained population raster - level distribution data for each city from the Global Human Settlement Layer (GHSL) (Corbane et al., 2019). These data are generated by disaggregating census or administrative unit data into grid cells and combining them with global building surface distribution, volume, and classification information. To ensure temporal proximity to the research period, we acquired the 2025 global population distribution forecast data from the GHSL platform. Subsequently, we extracted the necessary population feature vectors based on city boundaries and urban grids for further analysis.

3.2 Feature engineering

Referring to Woźniak and Szymański (2021), we utilized the H3 library from Uber to grid the cities, with each grid cell as a hexagon. In the H3 library, the grid resolution can be selected from levels 0 to 15, with higher resolutions yielding smaller grid areas and more feature vectors. We considered the impact of three typical resolutions on the model, with their parameters shown in Table 3. Since higher resolutions may also introduce more noise, selecting an appropriate grid resolution is crucial.

Considering that not all areas within a city are open to e-scooter operations (e.g., suburban or mountainous areas usually do not have e-scooter operational data), we focus on regions where shared e-scooters are frequently used. Based on the data of shared e-scooters and city boundaries, we first applied a convex hull algorithm to delineate the study area, filtering out areas of the city where e-scooters do not operate to avoid interference in the prediction process. This defined our area of interest (AOI), which ensures a balanced ratio of positive and

Table 2 POI types and descriptions from OSM

POI type	Description	POI type	Description
Aerialway	Gondolas, cable cars, and other aerial lifts	Other	Embassies, cemeteries, post offices, etc.
Airports	Airports and related aviation infrastructure	Roads_bike	Designated bicycle lanes and paths
Buildings	General-purpose buildings not otherwise categorized	Roads_drive	Roads and streets for motorized vehicles
Entertainment	Theaters, cinemas, and other cultural venues	Roads_walk	Sidewalks, footpaths, and pedestrian ways
Education	Schools, universities, and other educational institutions	Shops	All types of retail stores and commercial shops
Emergency	Emergency services and public safety facilities	Sports	Stadiums, gyms, and other sporting venues
Finances	Banks, ATMs, and currency exchange services	Sustenance	Restaurants, cafes, bars, and pubs
Healthcare	Hospitals, clinics, pharmacies, and medical facilities	Tourism	Hotels, museums, and other tourist facilities
Historic	Historical sites, monuments, and ruins	Transportation	Public transit stops, stations, and parking facilities
Leisure	Parks, plazas, playgrounds, and public leisure areas	Water	Rivers, lakes, canals, and other water bodies

Table 3 Parameters of different resolutions in H3

Resolution	Average Hexagon length (m)	Average Hexagon Area (m^2)
9	200.786148	105332.513
10	75.863783	15047.502
11	28.663897	2149.643

negative samples during model training. The AOI setting allows city managers to plan fixed e-scooter parking stations in any developing region of the city.

Next, we embedded OSM objects, specifically different categories of POI elements, into each grid as input features for the grid vectors. At the same time, we embedded the cluster centers as output labels into the grid vectors. To provide the classifier with more contextual information for prediction, we also included information about the surrounding neighborhood of each specific area in the embedded vectors. Typically, the neighborhood of an area consists of hexagons adjacent to the hexagon under study. Additionally, we examined the neighborhood size parameter, which corresponds to the number of rings of hexagons surrounding the study area and is treated as a hyperparameter for transfer learning. For the neighborhood feature vectors, we applied the diminishing average squared method to assign weights to them, where the weight of the n-th layer of the neighborhood is given by $1/(1+n)^2$. An example of this is shown in Fig. 2. The diminishing average squared weighting scheme is grounded in spatial decay principles, where quadratic decay provides stronger penalization of distant cells to emphasize local spatial dependencies while reducing noise from remote neighborhoods. We will discuss the application of this scheme in hyperparameter selection.

When collecting the grid feature vectors, we again used DBSCAN to obtain density clusters within the AOI. We labeled the grids containing cluster centers with a value of 1, indicating that these grids have the potential for planning e-scooter fixed parking stations. In contrast, grids without cluster centers were labeled as 0. Since the

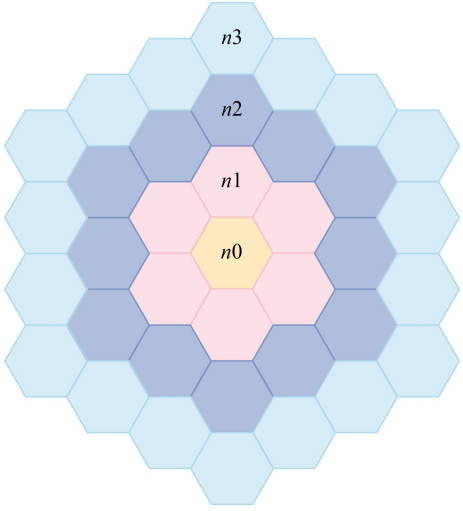

Fig. 2 An example of region neighborhoods of different sizes.

number of cluster centers is relatively small, this means that most areas do not have fixed parking stations. Therefore, we employed a limited negative sample set during the learning process and studied the impact of the ratio between positive and negative samples on prediction quality, treating this ratio as a hyperparameter for transfer learning.

Based on the data set mentioned above and feature processing, the prediction of e-scooter fixed parking stations can be formulated as a binary classification problem. We focused on three classic classification models: XGBoost, LightGBM, and Random Forest, and examined the influence of hyperparameters on cross-city transferability, selecting appropriate prediction models and hyperparameter settings during the study. Five classic metrics were used to evaluate the model's performance in the station prediction task, including accuracy, precision, F1 score, recall, and area under the curve (AUC) (Naidu et al., 2023).

3.3 Urban similarity matching

To further consider the transferability of the cities, we proposed a multidimensional urban feature similarity matching strategy based on socioeconomic characteristics, POI distribution features, and spatial structure features. First, we defined three feature‐dimension representations for each city. For city i, the base socioeconomic feature vector is $F_{\text{base}}^{(i)} = [G_i, P_i, E_i]$, where G_i, P_i and E_i are the geographic grouping code (Nordic = 1, Central = 2, Western = 3, Southern = 4, Eastern = 5), total population size, and economic development level (i.e., GDP per capita in purchasing power parity as a percentage of the EU27 average), respectively.

The functional layout of each city is quantified by its POI distribution features. For a city comprising N_i grid cells, $\rho_k^{(i)}$ is the average density of the k-th POI category, and $H^{(i)}$ is the city's POI diversity index. They are computed as specified in Eqs. (1) and (2), respectively.

$$\rho_k^{(i)} = \frac{1}{N_i}\sum_{j=1}^{N_i} POI_{k,j}^{(i)}, \tag{1}$$

$$H^{(i)} = -\sum_{k=1}^{K} p_k^{(i)} \log p_k^{(i)}, \tag{2}$$

$$p_k^{(i)} = \frac{\sum_{j=1}^{N_i} POI_{k,j}^{(i)}}{\sum_{k=1}^{K}\sum_{j=1}^{N_i} POI_{k,j}^{(i)}}, \tag{3}$$

where, $POI_{k,j}^{(i)}$ is the number of POIs of category k in the j-th grid cell of city i. The term $p_k^{(i)}$ (Eq. (3)) is the relative proportion of the k-th POI category, and K = 20 is the total number of POI categories. Consequently, the POI distribution feature vector is defined as $F_{poi}^{(i)} = [\rho_1^{(i)}, \rho_2^{(i)}, ..., \rho_K^{(i)}, H^{(i)}]$.

The spatial‐structure feature vector for city i is defined as $F_{\text{spatial}}^{(i)} = [D_{\text{pop}}^{(i)}, R_{\text{pos}}^{(i)}, \sigma_{\text{grid}}^{(i)}]$, where $D_{\text{pop}}^{(i)}$ is the average population density of city i at a uniform grid resolution, $R_{\text{pos}}^{(i)}$ is the parking-point grid ratio (i.e., the fraction of grid cells labeled as 1), and $\sigma_{\text{grid}}^{(i)}$ is the standard deviation of the grid-level population distribution, reflecting the equity of urban development.

Based on the definitions of these three feature vectors, we designed three similarity metrics to evaluate inter-city resemblance comprehensively. The socioeconomic similarity $S_{\text{econ}}(i,j)$, POI-distribution similarity $S_{\text{poi}}(i,j)$, and spatial-structure similarity $S_{\text{spatial}}(i,j)$ between cities i and j are defined in Eqs. (4)-(6).

$$S_{\text{econ}}(i,j) = \frac{1}{2}\left[\frac{1}{1+\left|E_i - E_j\right|} + \frac{\min(P_i, P_j)}{\max(P_i, P_j)}\right], \tag{4}$$

$$S_{\text{poi}}(i,j) = \frac{1}{2}\left[\frac{F_{\text{poi}}^{(i)} \cdot F_{\text{poi}}^{(j)}}{\|F_{\text{poi}}^{(i)}\| \cdot \|F_{\text{poi}}^{(j)}\|} + \left(1 - \frac{\left|H^{(i)} - H^{(j)}\right|}{\max\left(H^{(i)}, H^{(j)}\right)}\right)\right], \tag{5}$$

$$S_{\text{spatial}}(i,j) = \frac{1}{2}\left[\frac{\min\left(D_{\text{pop}}^{(i)}, D_{\text{pop}}^{(j)}\right)}{\max\left(D_{\text{pop}}^{(i)}, D_{\text{pop}}^{(j)}\right)} + \left(1 - \left|R_{\text{pos}}^{(i)} - R_{\text{pos}}^{(j)}\right|\right)\right]. \tag{6}$$

The overall similarity metric is defined as a weighted linear combination, i.e. $S_{\text{overall}}(i,j) = w_1 S_{\text{econ}}(i,j) + w_2 S_{\text{poi}}(i,j) + w_3 S_{\text{spatial}}(i,j)$, where $w_1 + w_2 + w_3 = 1$, and the weight parameters are determined via grid‐search optimization. To account for the influence of geographic proximity on urban similarity, we introduced a bonus term for cities within the same geographic grouping, as defined in Eq. (7). The geographic bonus mechanism is theoretically grounded in Tobler's first law of geography, which posits that spatially proximate entities exhibit stronger correlations than distant ones (Miller, 2004). The 1.1 × bonus coefficient was empirically determined through cross-validation experiments testing coefficients ranging from 1.0 to 1.2 with 0.05 increments. The moderate 10% enhancement provided by the 1.1 × factor effectively captures regional proximity benefits while avoiding overemphasis on geographic factors that could diminish the contribution of economic, POI, and spatial structure similarities.

$$S_{\text{final}}(i,j) = \begin{cases} 1.1 \times S_{\text{overall}}(i,j) & if \quad G_i = G_j \\ S_{\text{overall}}(i,j) & \text{otherwise} \end{cases}. \tag{7}$$

Using these similarity metrics, we conducted cross‐validation and performance evaluation for each city pair, ranked the source cities by their similarity scores and selected the top-K cities most suitable for transfer learning to the target city.

4 Results

4.1 Hyperparameter selection

Before the prediction, we calibrated the model's hyperparameters to select the most appropriate settings. The validation for this calibration task is based on the classified prediction of a single city. The ratio of the train set to the test set is 8:2.

First, we compared the impact of different grid resolutions and varying numbers of neighboring grid layers across three classification algorithms. As grid resolution increases, the grid side length and area decrease, which allows for a more precise representation of location areas. However, higher grid resolutions affect the ratio of positive to negative samples, further influencing data accuracy and computational resources. On the other hand, a greater number of neighboring grid layers means that the current central grid considers a wider neighborhood influence. However, too many layers may introduce excessive noise, interfering with the ability of city planners to select appropriate locations. In this study, we calculated the

performance metrics for XGBoost, LightGBM, and Random Forest across three grid resolutions (8, 9, 10) and six neighboring grid layers (0, 1, 2, 3, 4, 5), resulting in a total of 54 test cases, each repeated 100 times. For each grid resolution and number of neighboring layers, the results of the best-performing model are highlighted in bold. Among these, the optimal basic hyperparameters of the three models are presented in Table 4. We then averaged the results across the 25 cities, with the outcomes presented in Table 5.

The results in Table 5 indicate that model prediction quality tends to decline as grid resolution increases due to increased noise and data sparsity. Lower resolutions correspond to larger grid areas with more data per grid, facilitating spatial information capture. Additionally, increasing neighboring grid layers significantly improves prediction performance, highlighting the crucial role of spatial context information. Among the three models tested, Random Forest demonstrates superior performance. It can be attributed to its robustness to noise and data inconsistencies inherent in multi-city data sets, its effective handling of complex spatial feature interactions through bootstrap aggregating, and its built-in regularization that prevents overfitting in high-dimensional POI feature space with limited training samples per city.

To examine the relationship between grid resolution and city characteristics, we conducted stratified analysis across three population groups. Results show that large cities (> 1 million population) achieve optimal performance at resolutions 10-11, medium cities (0.5-1 million) perform best at resolution 10, while small cities (< 0.5 million) show optimal results at resolutions 9-10. This positive correlation reflects POI density effects on spatial analysis precision. Although optimal resolutions vary by

Table 4 Optimal basic hyperparameters of XGBoost, LightGBM, and Random Forest.

XGBoost	LightGBM	Random forest
eval_metric: logloss	boosting_type: gbdt	max_features: sqrt
n_estimators: 200	n_estimators: 200	n_estimators: 200
max_depth: 6	max_depth: 6	max_depth: 10
learning_rate: 0.05	learning_rate: 0.05	min_samples_split: 5
colsample_bytree: 0.8	num_leaves: 31	min_samples_leaf: 2
Subsample: 0.8	class_weight: balanced	class_weight: balanced

Table 5 Prediction results for 25 cities at different resolutions, neighboring size, and models (The best model chosen for each resolution and neighborhood size has been highlighted).

Hex	Neigh Size	XGBoost					LightGBM					Random Forest				
		Accu	Preci	Recall	F1	AUC	Accu	Preci	Recall	F1	AUC	Accu	Preci	Recall	F1	AUC
9	0	0.8128	0.7876	0.8110	0.7949	0.8953	0.8175	0.7763	0.8475	0.8059	0.8957	**0.8264**	**0.7798**	**0.8645**	**0.8166**	**0.9028**
	1	0.8437	0.8106	0.8623	0.8331	0.9219	0.8435	0.8036	0.8703	0.8330	0.9193	**0.8499**	**0.8085**	**0.8799**	**0.8401**	**0.9236**
	2	**0.8574**	**0.8254**	**0.8788**	**0.8485**	**0.9332**	0.8557	0.8193	0.8806	0.8463	0.9309	0.8596	0.8208	0.8876	0.8506	0.9321
	3	**0.8649**	**0.8320**	**0.8920**	**0.8582**	**0.9393**	0.8639	0.8269	0.8941	0.8566	0.9367	0.8648	0.8285	0.8927	0.8568	0.9362
	4	**0.8694**	**0.8346**	**0.9014**	**0.8638**	**0.9433**	0.8666	0.8292	0.8994	0.8602	0.9399	0.8688	0.8321	0.8995	0.8618	0.9404
	5	0.8702	0.8314	0.9019	0.8644	0.9418	**0.8791**	**0.8315**	**0.9024**	**0.8626**	**0.9422**	0.8686	0.8319	0.8992	0.8616	0.9409
10	0	0.7701	0.6131	0.8205	0.6938	0.8722	0.7639	0.5969	0.8612	0.6992	0.8746	**0.7665**	**0.5967**	**0.8731**	**0.7038**	**0.8773**
	1	0.7931	0.6357	0.8534	0.7238	0.8935	0.7880	0.6249	0.8732	0.7241	0.8938	**0.7936**	**0.6317**	**0.8772**	**0.7303**	**0.8965**
	2	0.8066	0.6520	0.8684	0.7408	0.9037	0.8020	0.6430	0.8796	0.7392	0.9030	**0.8068**	**0.6501**	**0.8797**	**0.7441**	**0.9044**
	3	0.8160	0.6649	0.8770	0.7526	0.9113	0.8109	0.6552	0.8860	0.7499	0.9095	**0.8164**	**0.6640**	**0.8841**	**0.7550**	**0.9106**
	4	0.8223	0.6737	0.8842	0.7612	0.9165	0.8172	0.6644	0.8899	0.7574	0.9145	**0.8225**	**0.6732**	**0.8870**	**0.7623**	**0.9145**
	5	**0.8275**	**0.6803**	**0.8913**	**0.7684**	**0.9196**	0.8216	0.6699	0.8977	0.7639	0.9171	0.8275	0.6805	0.8903	0.7683	0.9169
11	0	0.7610	0.5652	0.8173	0.6626	0.8542	0.7509	0.5522	0.8504	0.6645	0.8575	**0.7518**	**0.5515**	**0.8505**	**0.6646**	**0.8584**
	1	0.7713	0.5731	0.8571	0.6831	0.8771	0.7640	0.5619	0.8746	0.6817	0.8779	**0.7648**	**0.5625**	**0.8811**	**0.6841**	**0.8799**
	2	0.7789	0.5821	0.8650	0.6931	0.8847	0.7739	0.5744	0.8776	0.6918	0.8850	**0.7763**	**0.5769**	**0.8799**	**0.6946**	**0.8862**
	3	0.7938	0.5876	0.8725	0.6998	0.8899	0.7796	0.5812	0.8831	0.6986	0.8898	**0.7830**	**0.5858**	**0.8826**	**0.7018**	**0.8907**
	4	**0.7885**	**0.5933**	**0.8791**	**0.7062**	**0.8943**	0.7841	0.5866	0.8870	0.7038	0.8936	0.7885	0.5928	0.8847	0.7076	0.8942
	5	**0.7924**	**0.5978**	**0.8829**	**0.7108**	**0.8974**	0.7977	0.5907	0.8907	0.7082	0.8964	0.7925	0.5976	0.8866	0.7119	0.8967

city size, resolution 10 provides the best balance between accuracy and practical applicability across most cities in our data set.

Although model performance at resolution 9 is slightly better overall, resolution 10 was selected as it provides the best balance between accuracy and practical applicability across most cities in our data set. Resolution 10 offers higher spatial precision for capturing local features while maintaining prediction performance suitable for rapid deployment, enabling more refined management and precise decision-making for city planners and operators.

Based on the above analysis, the final combination of hyperparameters we selected is: resolution 10, grid layers 5, and the Random Forest model. Under this combination, Fig. 3 presents the density results of evaluation metrics for the five best-performing cities or regions (Zurich, Stjordal, Bari, Innsbruck, Basel) and the five worst-performing ones (Madrid, Utrecht, Krakow, Budapest, CASGBS). The results show that under the specified parameters, the predictive performance of these cities is satisfactory.

To validate our neighborhood weighting function, we compared four schemes: equal weighting ($w_n = 1$), diminishing averaging ($w_n = 1/(n+1)$), exponential decay ($w_n = \exp(-0.5n)$), and diminishing average squared ($w_n = 1/(n+1)^2$). Table 6 presents the comparative results across all cities. While all methods show relatively similar performance due to the controlled single-city validation environment, the diminishing average squared method achieves the best F1-score (0.8281), demonstrating an optimal balance between precision and recall. The modest performance differences reflect that neighborhood weighting effects become more pronounced in cross-city

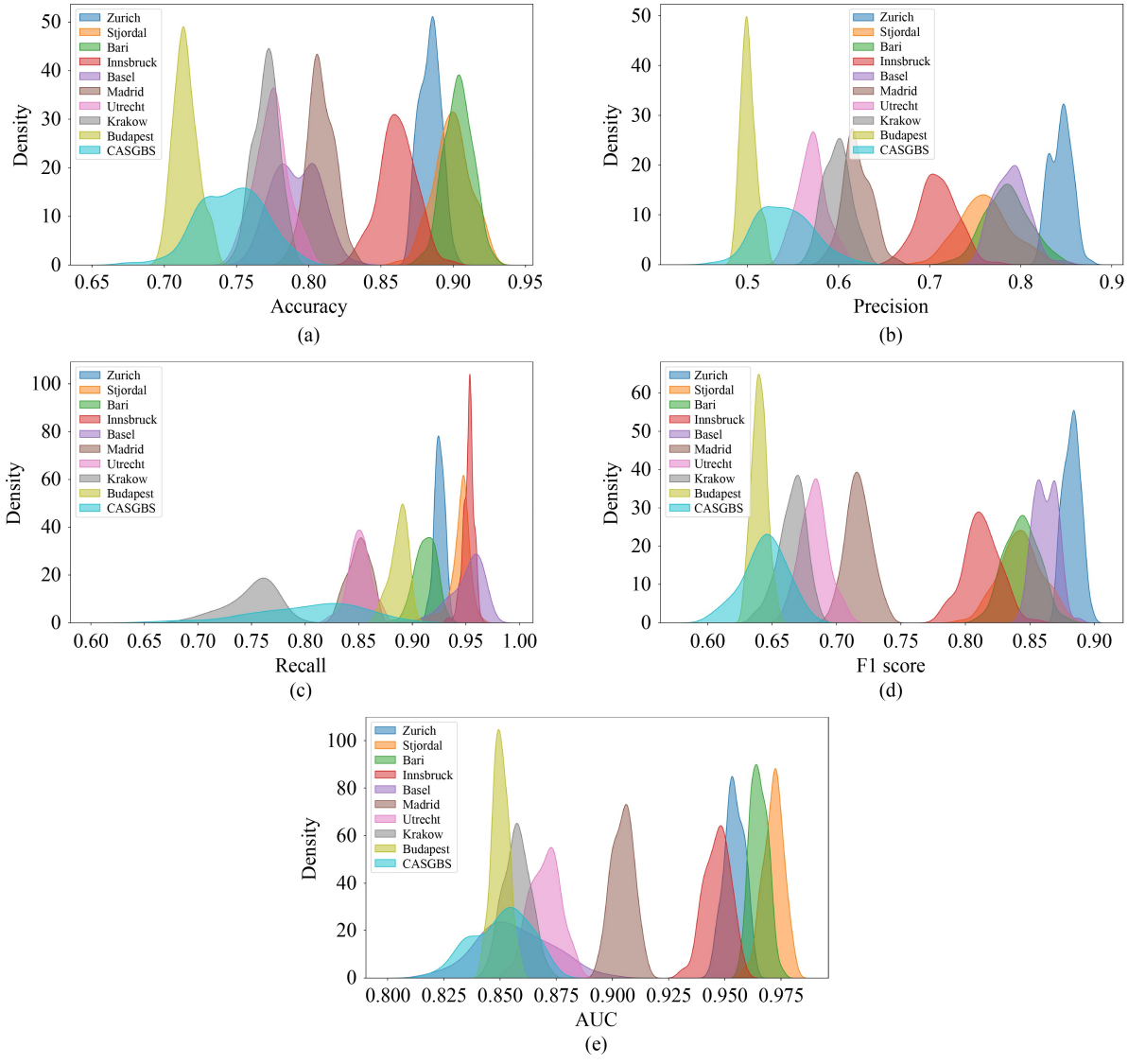

Fig. 3 The density results of the five best cities and the five worst cities: (a) Accuracy; (b) Precision; (c) Recall; (d) F1 score and (e) AUC.

Table 6 Performance comparison of different neighborhood weighting schemes.

	Accuracy	Precision	Recall	F1 score	AUC
Equal weighting	0.9022	0.7652	0.9001	0.8243	0.9628
Exponential decay	**0.9046**	0.7719	0.8992	0.8264	0.9638
Diminishing averaging	0.9045	**0.7725**	0.8957	0.8272	0.9634
Diminishing averaging squared	**0.9046**	0.7691	**0.9018**	**0.8281**	**0.9640**

transfer scenarios where spatial heterogeneity is greater.

It should be noted that the relatively high-performance values across all methods reflect the controlled single-city validation environment used for hyperparameter calibration, with the true discriminative power of different approaches becoming more apparent in subsequent cross-city transfer experiments.

4.2 Single-source transfer

Based on the above-determined model hyperparameter combination, we conducted cross-city transfer predictions for the 25 studied cities to verify whether models trained in source cities can be effectively applied to predict parking stations in target cities. The results of all cross-validation metrics are presented in Fig. 4. In transfer prediction, the validation set includes input feature vectors for all grids in the target cities, resulting in an imbalance between grids with and without stations. This imbalance leads to relatively high overall Accuracy and AUC values for the models. In most cases, the Precision and F1 scores of the models are relatively low, as they predicted many city grids without stations, although they generally remained above 0.6.

Moreover, Recall reflects the model's ability to identify positive classes, and its results vary between 0 and 1. Therefore, we specifically generated a heatmap of Recall values for all cities in the cross-validation process, as shown in Fig. 5. It shows that when used as target cities, Berlin, Hamburg, Budapest, Stjordal, Munich, Boras, and Varberg reported relatively poor prediction results. This is due to the large number of grid features within the AOI of these cities, making it difficult for models trained on smaller samples to predict large data sets. In contrast, when these cities were used as source cities, they often enabled the target cities to achieve higher Recall values. Additionally, when Madrid, Krakow, Wroclaw, Gdansk, and CASGBS were used as source cities, the Recall performance for predicting target cities was relatively poor. On the one hand, this is related to the imbalance of positive and negative samples within the AOI of these cities, which led to poor station prediction performance. On the other hand, these cities may differ from others in terms of shared mobility penetration, urban planning, and infrastructure, although this has not yet been conclusively demonstrated in spatial features.

To further investigate the reasons for the aforementioned

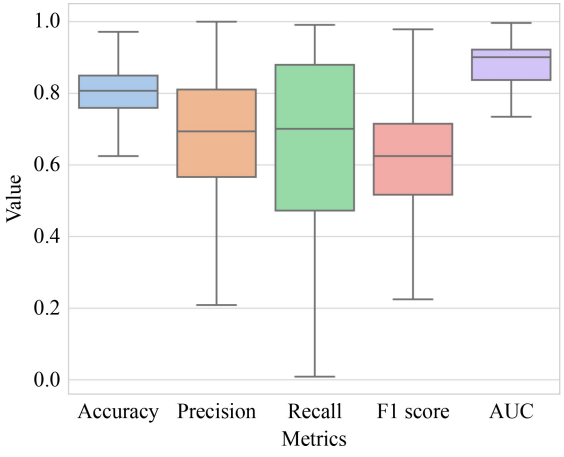

Fig. 4 Box plot results for five metrics.

low recall, we analyzed the relationship between the spatial complexity of relevant cities and recall from the perspective of urban complexity. Spatial complexity consists of four key indicators, including (1) the multi-center index, which measures the dispersion of high-density areas, (2) the coefficient of variation of POI density distribution, (3) the coefficient of variation of population density distribution, and (4) the POI type diversity score based on the Shannon index (Yue et al., 2017). Additionally, the number of grids within the AOI reflects the impact of city size. Ultimately, our quantitative analysis reveals a significant negative correlation between urban complexity and recall performance (Pearson r=−0.5761, p=0.0026), confirming that cities with complex spatial structures, characterized by multi-center layouts, heterogeneous POI distribution, and diverse functional areas, pose greater challenges to cross-city knowledge transfer. As shown in Fig. 6, cities such as Varberg, Hamburg, and Stjordal exhibit high complexity scores and poor recall performance, while simpler city structures facilitate more effective transfer learning. This finding confirms that the poor performance of large cities is not only due to data volume issues but also to fundamental urban spatial complexity, which complicates cross-city pattern recognition and knowledge generalization.

Our analysis for poor-performing cities such as Varberg, Hamburg, and Stjordal reveals three primary failure patterns: (1) Data quality issues: Cities with sparse or inconsistent e-scooter operational data lead to unreliable ground truth labels, as observed in Varberg, where

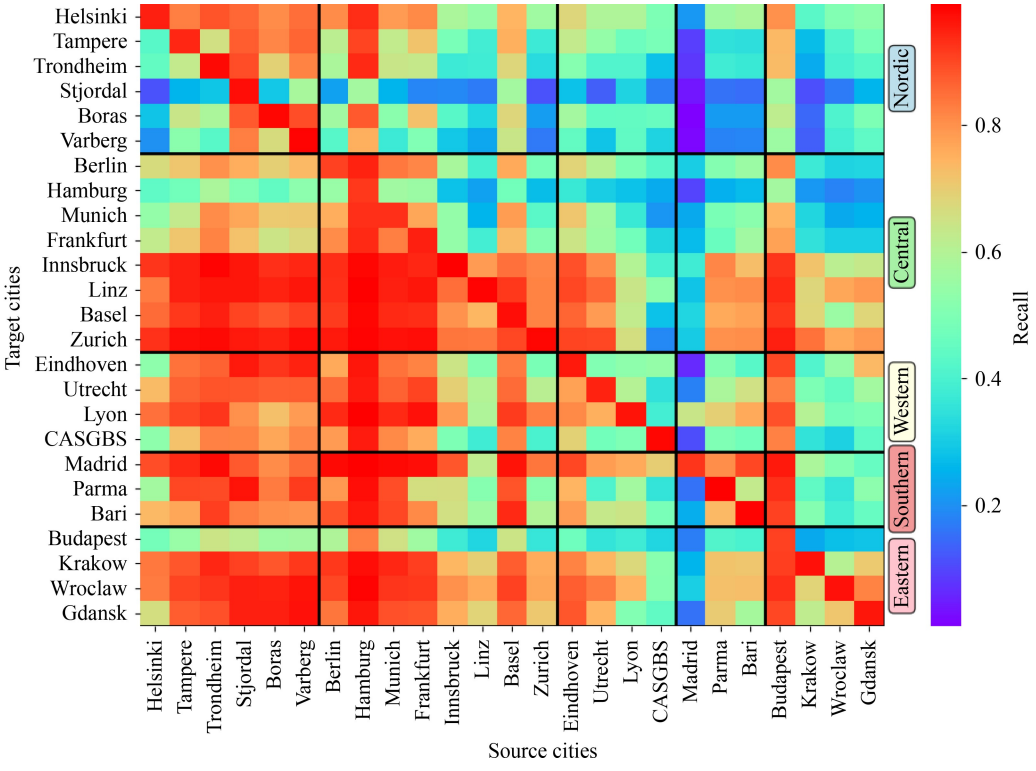

Fig. 5 Recall metric in cross-city prediction.

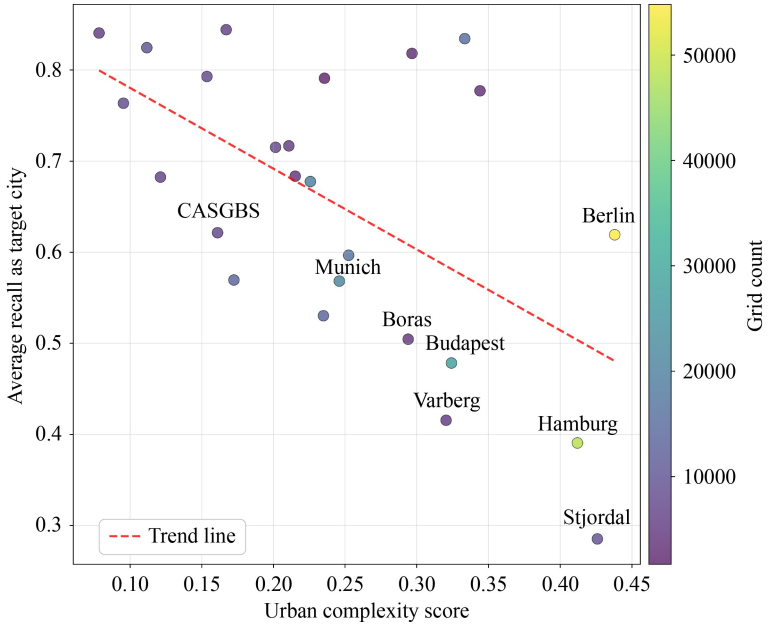

Fig. 6 Urban complexity vs transfer learning recall oerformance.

limited operational coverage creates insufficient positive samples for effective training. (2) Urban complexity mismatch: Cities with extremely high spatial complexity scores (> 0.3) exhibit fundamental structural differences that challenge knowledge transfer, particularly those with multiple urban centers or irregular development patterns. (3) Economic-spatial disconnect: Cities where economic classification based on regional averages poorly reflects local urban development patterns show reduced transferability. Based on these findings, we proposed targeted improvement strategies. For data-sparse cities, we recommend hybrid approaches that combine our framework with local pilot programs to build reliable data sets gradually. For highly complex cities, ensemble methods

integrating multiple source cities with different urban characteristics may improve robustness. For cities with classification uncertainties, sensitivity analysis and multi-scenario validation should be conducted before deployment.

4.3 Multi-source group transfer

To investigate the effects of these three factors on cross-city station prediction performance, we conducted intra-group tests. We examined the impact of urban geographic location, population size, and economic level on the prediction of e-scooter parking deployment. The grouping schemes for the various categories are detailed in Table 1. Specifically, within each category and for each group of cities, each city was treated in turn as the target city, while all other cities in the group (excluding the target) served as source cities. Additionally, we utilize the F1 Score and AUC as primary metrics for a more comprehensive evaluation. F1 Score provides a balanced assessment of both precision and recall, which is crucial for practical deployment where both false positives (unnecessary stations) and false negatives (missed opportunities) incur costs. AUC offers a threshold-independent evaluation that better reflects the model's overall discriminative ability across different operational scenarios. This shift in evaluation focus aligns with the practical requirements of cross-city transfer learning, where balanced performance is more valuable than maximizing any single metric.

Figure 7 illustrates the distribution of F1 scores for each city group under the three classification schemes. When performing cross-city transfer based on geographic region, the Central European group achieved the highest performance, with an average F1 score of 0.75. Within this group, Basel and Zurich were particularly outstanding, reflecting the homogeneity in urban planning and infrastructure among developed economies such as Germany, Austria, and Switzerland. The Nordic group exhibited moderate performance (average 0.609), the Eastern European group remained stable (average 0.624), and the Southern European group performed the weakest (average 0.459), indicating that geographic similarity has a significant effect on transfer learning efficacy. When conducting cross-city transfers based on population size, all city-size categories yielded satisfactory results, suggesting that similar population scales facilitate the prediction of e-scooter parking hotspots. Accordingly, planners in the target city may initially draw on deployment

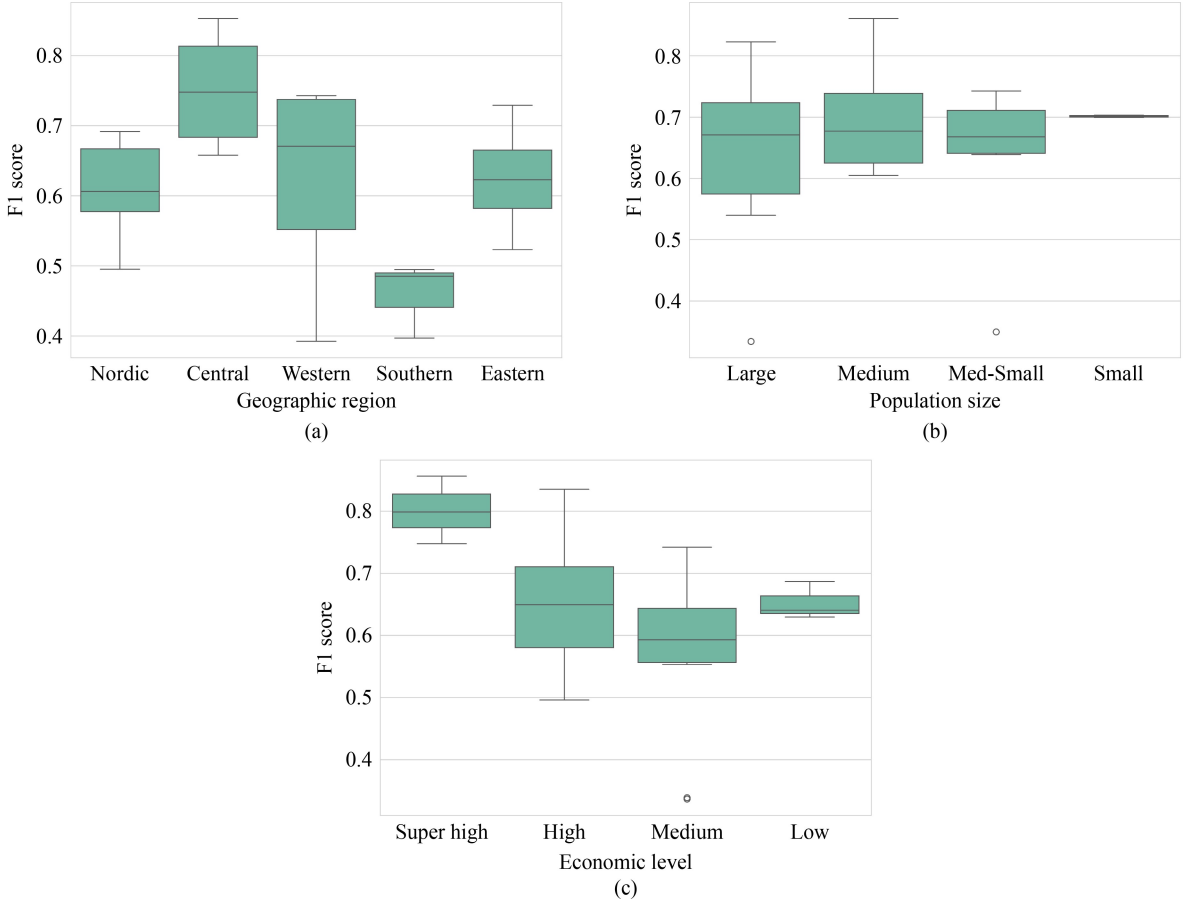

Fig. 7 F1 score distribution of three classifications: (a) Geographic groups; (b) Population groups; and (c) Economic groups.

experiences from cities with comparable population sizes. Finally, when using economic level as the basis for transfer, the very-high-income group demonstrated exceptional performance, with an average F1 score of 0.801, underscoring the decisive role of economic prosperity in urban infrastructure quality, data reliability, and planning rigor. The low-income group maintained stable performance, while the high- and middle-income groups, despite comprising the largest number of cities, exhibited greater internal heterogeneity—thereby providing a clear economic threshold reference for deployments in new urban contexts.

Figure 8 presents the average AUC results for each city group under the three classification schemes. It can be observed that, across all categories, the group-level averages consistently demonstrate high performance. This indicates that the employed POI features and spatial embedding techniques effectively capture the latent spatial patterns of parking demand. Regardless of variations in urban characteristics, the combination of 20 POI categories derived from OSM data provides a robust discriminative foundation for the model, suggesting that the spatial distribution patterns of functional zones, such as commercial, transportation, and residential areas, exhibit considerable consistency across European cities. However, the relatively high AUC values coupled with lower F1 scores imply that, although the model possesses strong ranking capability, there remain challenges in accurately pinpointing the optimal parking locations.

Table 7 presents the overall performance of intra-group transfer learning under the three classification schemes, where the numerical values for the best and worst performers are the F1 scores. The analysis of individual city performance reveals several noteworthy patterns. Basel emerges as the top performer across all classification systems, reflecting the combined advantages of being a medium-sized, very-high-income city located in Central Europe. In contrast, CASGBS consistently ranks lowest across all groupings, indicating the potential influence of its unique urban characteristics and possible data quality issues. Varberg exhibits strong group dependency, achieving the highest performance within the population-based grouping. Still, the lowest within the economic-based grouping, highlighting the multidimensional

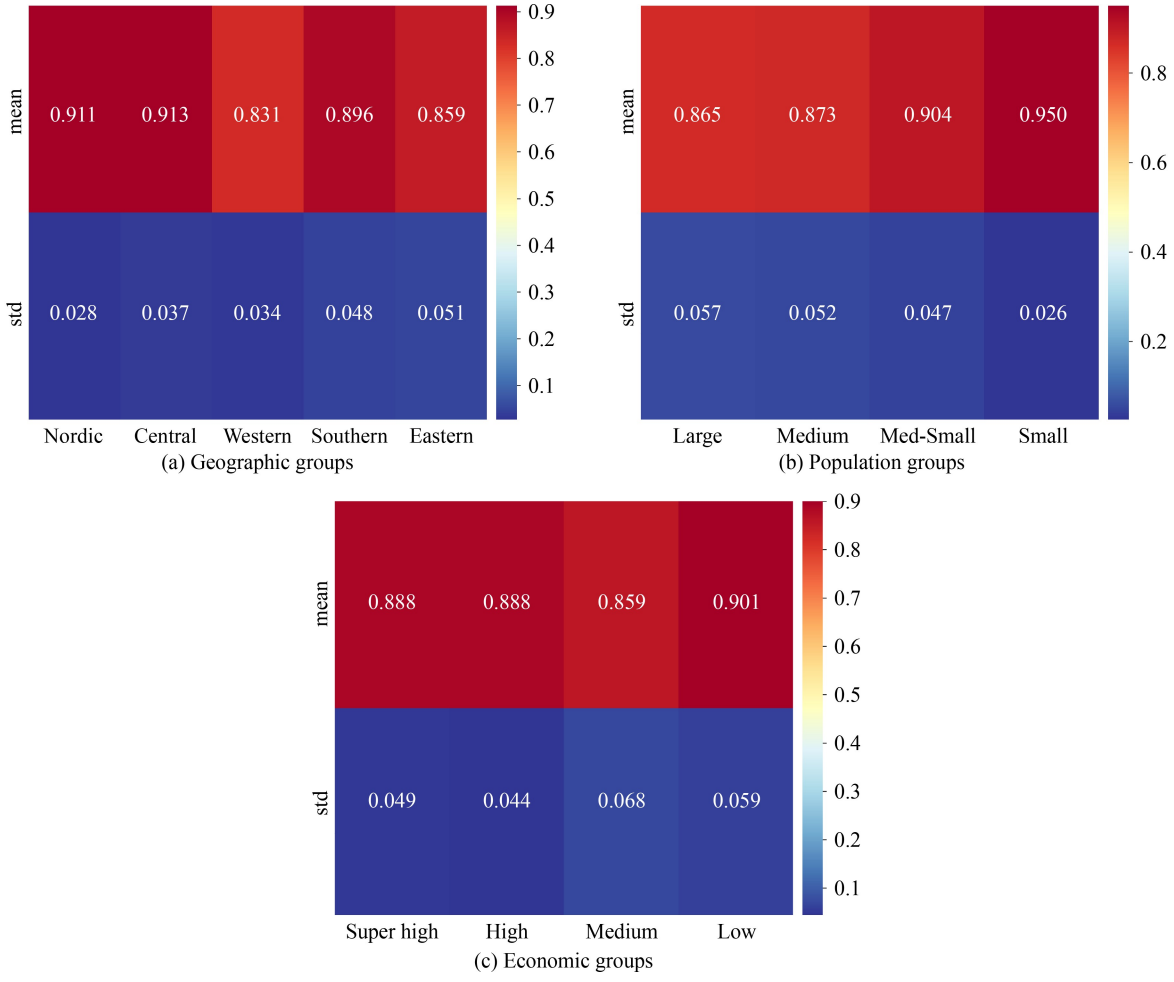

Fig. 8 Average AUC of three classifications: (a) Geographic groups; (b) Population groups; and (c) Economic groups.

Table 7 Performance comparison of different neighborhood weighting schemes

Classification	Group	Cities	Avg F1 ± Std	Avg AUC ± Std	Best performer	Worst performer
Geography	Nordic	6	0.609 ± 0.074	0.911 ± 0.028	Boras (0.692)	Helsinki (0.495)
	Central	8	0.750 ± 0.077	0.913 ± 0.037	Basel (0.853)	Linz (0.658)
	Western	4	0.619 ± 0.164	0.831 ± 0.048	Eindhoven (0.743)	CASGBS (0.392)
	Southern	3	0.459 ± 0.054	0.896 ± 0.048	Parma (0.495)	Madrid (0.397)
	Eastern	4	0.624 ± 0.086	0.859 ± 0.051	Gdansk (0.729)	Budapest (0.523)
Population	Large	8	0.639 ± 0.155	0.865 ± 0.057	Zurich (0.822)	Madrid (0.334)
	Medium	6	0.698 ± 0.097	0.873 ± 0.052	Basel (0.861)	Utrecht (0.605)
	Med-Small	9	0.646 ± 0.118	0.904 ± 0.047	Innsbruck (0.742)	CASGBS (0.350)
	Small	2	0.701 ± 0.003	0.950 ± 0.026	Varberg (0.703)	Stjordal (0.699)
Economy	Super-high	3	0.801 ± 0.054	0.888 ± 0.049	Basel (0.856)	Frankfurt (0.748)
	High	7	0.652 ± 0.112	0.888 ± 0.044	Zurich (0.835)	Helsinki (0.496)
	Medium	12	0.579 ± 0.127	0.859 ± 0.068	Innsbruck (0.742)	CASGBS (0.336)
	Low	3	0.652 ± 0.030	0.901 ± 0.059	Bari (0.687)	Varberg (0.629)

complexity of urban attributes and their impact on transfer learning outcomes.

It should be noted that the economic-level classification for some cities used regional/national averages. To assess the robustness of our economic grouping results to classification uncertainties, we conducted a sensitivity analysis on two example cities with approximated economic data: Tampere and Stjordal. We tested three alternative scenarios by reassigning them to the high-income group and re-evaluated the intra-group transfer performance, with results shown in Table 8. The results indicate that across different test scenarios, the average F1-score of the low group, medium group, and high group varies within the range of 0.652–0.676, 0.579–0.590, and 0.627–0.652, respectively, demonstrating that classification adjustments have a limited impact on intra-group performance. Although individual cities show performance fluctuations due to group reassignment, the overall superiority of economic similarity-based grouping remains consistent, validating the robustness of our economic classification approach.

4.4 Validation of city similarity matching

In this section, we further validate the matching efficacy across different city classification features to select the optimal set of source cities for each target city. Table 9 summarizes, for each target city, the three most similar source cities. The weight parameters optimized via grid search are $w_1 = 0.4$, $w_2 = 0.1$, and $w_3 = 0.5$. The weight parameters were determined through systematic grid search optimization across 36 feasible combinations. As shown in Fig. 9, this optimal combination achieved the highest average F1-score of 0.672 across all cities, demonstrating that spatial structure similarity is the most influential factor for cross-city knowledge transfer, followed by economic-population similarity, while POI distribution similarity provides complementary information.

Results in Table 9 indicate that the highest-similarity city pair is Wroclaw–Krakow, achieving an overall similarity score of 0.957. Among all TOP-1 selections, Zurich and Wroclaw occur most frequently, suggesting that these cities yield superior transfer predictions when treated as targets. Furthermore, based on the findings in Table 9, we conducted comparative predictions for each target city using their TOP-3 and TOP-5 similar cities. The benchmark for comparison is the average performance obtained under the geographic-location, population-size, and economic-level schemes, as illustrated in Fig. 10.

The results in Fig. 10 demonstrate that the TOP-3 similarity-matching strategy generally achieves higher average

Table 8 Sensitivity analysis results for the economic classification of Tampere and Stjordal.

Test case	Avg F1 ± Std of low	Avg F1 ± Std of medium	Avg F1 ± Std of high	F1 of Tampere	F1 of Stjordal
Original	0.652 ± 0.030	0.579 ± 0.127	0.652 ± 0.112	0.6329	0.5576
Case 1	0.676 ± 0.033	0.580 ± 0.127	0.652 ± 0.112	0.6245	0.5362
Case 2	0.652 ± 0.030	0.587 ± 0.126	0.627 ± 0.113	0.6343	0.4787
Case 3	0.676 ± 0.033	0.590 ± 0.132	0.627 ± 0.113	0.6245	0.4787

Notes: Cases 1 and 2 indicate that only Tampere is divided into the low group, and only Stjordal is divided into the high group from the medium group; Case 3 shows that two cities are regrouped at the same time.

Table 9 Top-5 most similar source cities and their overall similarity scores

Target city	TOP-5 similar cities (Comprehensive similarity)				
	1	2	3	4	5
Helsinki	Hamburg (0.823)	Parma (0.823)	Wroclaw (0.750)	Budapest (0.744)	Tampere (0.734)
Tampere	Trondheim (0.896)	Boras (0.881)	CASGBS (0.793)	Bari (0.764)	Helsinki (0.734)
Trondheim	Boras (0.914)	Tampere (0.896)	Varberg (0.737)	Linz (0.734)	Helsinki (0.725)
Stjordal	Varberg (0.733)	Trondheim (0.641)	Boras (0.615)	Helsinki (0.576)	Tampere (0.569)
Boras	Trondheim (0.914)	Tampere (0.881)	Innsbruck (0.738)	Varberg (0.736)	Helsinki (0.694)
Varberg	Trondheim (0.737)	Boras (0.736)	Stjordal (0.733)	Tampere (0.715)	Helsinki (0.597)
Berlin	Budapest (0.833)	Zurich (0.808)	Innsbruck (0.795)	Krakow (0.795)	Hamburg (0.782)
Hamburg	Zurich (0.866)	Budapest (0.854)	Helsinki (0.823)	Linz (0.809)	Berlin (0.782)
Munich	Zurich (0.902)	Basel (0.799)	Budapest (0.756)	Hamburg (0.746)	Frankfurt (0.738)
Frankfurt	Utrecht (0.853)	Wroclaw (0.851)	Parma (0.796)	Hamburg (0.778)	Linz (0.775)
Innsbruck	Linz (0.922)	Berlin (0.795)	CASGBS (0.776)	Frankfurt (0.771)	Wroclaw (0.770)
Linz	Innsbruck (0.922)	Eindhoven (0.848)	Hamburg (0.809)	Utrecht (0.797)	CASGBS (0.792)
Basel	Munich (0.799)	Frankfurt (0.728)	Zurich (0.686)	Utrecht (0.655)	Krakow (0.650)
Zurich	Munich (0.902)	Hamburg (0.866)	Budapest (0.862)	Berlin (0.808)	Krakow (0.764)
Eindhoven	Utrecht (0.890)	CASGBS (0.883)	Linz (0.848)	Parma (0.819)	Gdansk (0.804)
Utrecht	Wroclaw (0.900)	Eindhoven (0.890)	Frankfurt (0.853)	Parma (0.841)	CASGBS (0.838)
Lyon	Zurich (0.726)	Budapest (0.717)	Munich (0.707)	Krakow (0.669)	Madrid (0.663)
CASGBS	Bari (0.897)	Eindhoven (0.883)	Utrecht (0.838)	Parma (0.811)	Gdansk (0.805)
Madrid	Berlin (0.682)	Lyon (0.663)	Parma (0.637)	Krakow (0.600)	Bari (0.597)
Parma	Wroclaw (0.896)	Utrecht (0.841)	Bari (0.833)	Helsinki (0.823)	Eindhoven (0.819)
Bari	CASGBS (0.897)	Parma (0.833)	Gdansk (0.816)	Wroclaw (0.815)	Utrecht (0.789)
Budapest	Zurich (0.862)	Hamburg (0.854)	Krakow (0.852)	Berlin (0.833)	Wroclaw (0.829)
Krakow	Wroclaw (0.957)	Budapest (0.852)	Utrecht (0.823)	Parma (0.815)	Gdansk (0.798)
Wroclaw	Krakow (0.957)	Utrecht (0.900)	Parma (0.896)	Gdansk (0.878)	Frankfurt (0.851)
Gdansk	Wroclaw (0.878)	Bari (0.816)	CASGBS (0.805)	Eindhoven (0.804)	Krakow (0.798)

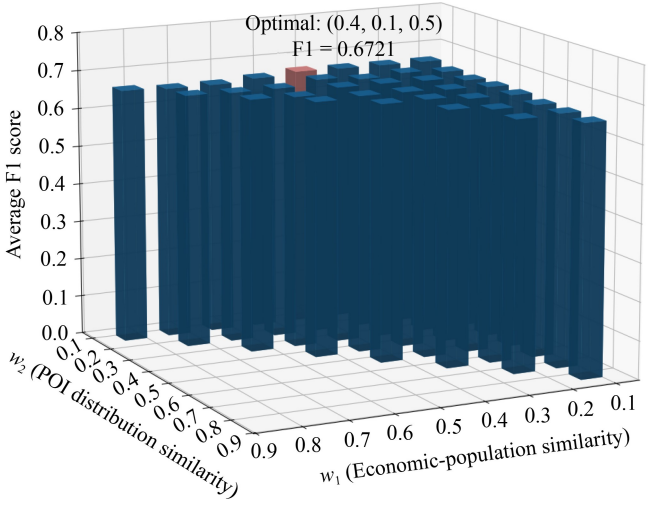

Fig. 9 Weight optimization results in city similarity measurement.

F1 scores compared to the geographic, population-based, and economic-level grouping methods. Although some cities may underperform relative to one of the three grouping schemes, the TOP-3 approach exhibits superior stability and generalization across diverse urban contexts, yielding overall better predictive performance. And compared to conventional geographical, demographic, and economic grouping, the TOP-3 strategy has improved the predictive performance of more cities. It is noteworthy that, despite leveraging a larger pool of source cities, the TOP-5 strategy underperforms slightly relative to TOP-3, indicating that precise similarity matching is more effective than the mere accumulation of information; incorporating too many source cities may introduce noise and degrade prediction accuracy.

The superior performance of the TOP-3 over the TOP-5 strategy reveals essential insights about information redundancy and similarity thresholds in multi-source transfer learning. Analysis of similarity score distributions shows that expanding beyond TOP-3 often introduces source cities with similarity scores below 0.82, which tend to contribute noise rather than functional patterns.

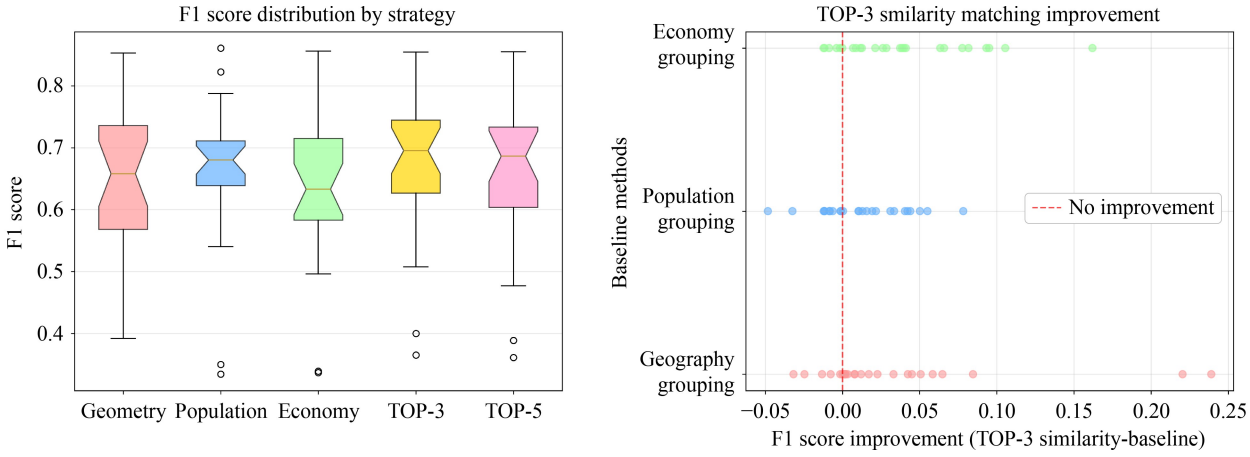

Fig. 10 Distribution of F1 scores for all cities under the five strategies (left) and the relative improvement afforded by the TOP-3 matching strategy over each grouping scheme (right).

This suggests an optimal balance exists between source diversity and similarity: while moderate diversity (TOP-3) provides sufficient pattern variation for robust transfer learning, excessive diversity (TOP-5) introduces information conflicts and redundancy that degrade performance. The phenomenon suggests that effective cross-city transfer necessitates careful curation of source cities, rather than merely maximizing the number of sources.

4.5 Practical application case study

To demonstrate the practical deployment of our framework, we present a step-by-step application workflow for implementing our methodology in a new target city seeking to establish e-scooter parking infrastructure. This workflow emphasizes the need for local adaptation while maintaining the core methodological framework.

Step 1: Data Collection – Obtain POI data from OpenStreetMap using Overpass API, obtain city-level total population statistics from World Population Review, download population raster data from GHSL platform, and collect economic indicators from regional statistical databases. For cities outside our study context, adapt POI categories to reflect local urban characteristics.

Step 2: Preprocessing – Apply H3 hexagonal gridding, extract AOI using the convex hull algorithm, and embed neighborhood features with a multi-layer weighting scheme.

Step 3: City Similarity Calculation – Compute similarities using our multi-dimensional framework. Note that optimal weights should be re-determined through grid search optimization based on available source cities and local validation data, as our weights are specific to European urban contexts.

Step 4: Source City Selection – Identify the TOP-3 most similar cities through systematic ranking. The similarity threshold should be empirically determined based on the available source city pool and cross-validation performance.

Step 5: Model Training and Prediction – Select optimal algorithm through hyperparameter tuning on local validation data, as model performance may vary with different urban contexts.

Step 6: Result Interpretation – Determine probability thresholds through pilot testing and local stakeholder consultation, as optimal deployment strategies depend on local policy constraints and operational requirements.

5 Conclusions

This study proposes a cross-city transfer learning method for predicting shared e-scooter parking stations, enabling rapid infrastructure planning in new cities through the integration of operational data from 25 European cities and OpenStreetMap spatial data. The developed framework addresses the critical challenge of deploying e-scooter parking infrastructure without extensive local data collection by leveraging knowledge transfer from established markets. Through systematic feature engineering incorporating hexagonal grid discretization, POI data embedding, and neighborhood influence modeling, the method transforms complex urban spatial patterns into learnable representations suitable for cross-city knowledge transfer.

The empirical findings reveal several critical patterns for practical implementation. Cities with similar economic development levels exhibit stronger knowledge transferability, suggesting that purchasing power and infrastructure investment capacity fundamentally shape e-scooter usage patterns. The superior performance of medium-sized cities indicates that targeted deployment strategies should prioritize these markets over large metropolitan areas where complexity and scale introduce additional prediction challenges. Geographic proximity shows a meaningful but secondary influence. Addition-

ally, we recommend that urban planners adopt the TOP-3 similarity-matching strategy when designing e-scooter parking infrastructure for new cities, rather than relying solely on traditional geographic proximity or single economic-indicator groupings. For shared-mobility operators, selecting the three most analogous existing cities as experiential references during market expansion cannot only enhance prediction accuracy but also control data‐collection and analysis costs. Moreover, policymakers should consider establishing a multidimensional urban feature database—encompassing POI distributions, spatial structure metrics, and socio-economic characteristics—to support coordinated policymaking and best‐practice dissemination among similar cities, thereby improving the overall efficiency and precision of shared-mobility infrastructure planning.

From a policy and operational perspective, these findings support several strategic recommendations for stakeholders. E-scooter operators should prioritize deployment in economically advanced cities where prediction accuracy is highest and infrastructure investment is most likely to yield positive returns. The demonstrated effectiveness of medium-sized cities suggests these markets should serve as priority pilot regions rather than pursuing immediate large-scale metropolitan deployments. Geographic clustering effects indicate that successful implementation in one region can effectively inform expansion to neighboring areas. For urban planners, the multi-dimensional similarity framework provides a systematic approach to learning from comparable cities rather than relying solely on local pilot programs or generic best practices.

It should be noted that the foundational methods used in this study have certain limitations. The 20 POI categories derived from OpenStreetMap were designed and validated for European urban contexts, and their applicability to Asian or African cities may be limited. These categories may not adequately capture unique urban features such as informal settlements or different mixed-use development patterns common in non-European cities. Additionally, cultural differences in mobility patterns and infrastructure development could affect the transferability of our findings. Future applications to non-European contexts would require adaptation of the POI categorization scheme to reflect local urban characteristics and potentially the incorporation of additional data sources that better represent diverse urban development patterns. The economic classification approach, while generally robust, relies on approximations for some cities lacking direct NUTS 3 data, which may introduce classification uncertainties. Additional limitations include temporal constraints, as our data represents summer usage patterns, which may not fully capture seasonal variations in e-scooter demand. Furthermore, the rapidly evolving nature of the e-scooter industry—including changing user behaviors, policy environments, and operational strategies—may require periodic model updates to maintain effectiveness. Future research should consider incorporating temporal dynamics and policy factors as additional urban characteristic dimensions to enhance the framework's adaptability to industry evolution. We will incorporate more comprehensive, multidimensional urban matching characteristics and apply advanced deep learning techniques or large language models to enhance the precision of transfer learning for target cities.

Data availability statement This study is based on publicly available data sources including: (1) OpenStreetMap (openstreetmap.org) for POI data accessed through the Overpass API; (2) Global Human Settlement Layer (ghsl.jrc.ec.europa.eu) for population distribution raster data; (3) World Population Review (worldpopulationreview.com/cities/continent/) for city-level total population statistics; (4) Eurostat Regional Database (ec.europa.eu/eurostat/web/main/data/database) for purchasing power standards and economic classification data; and (5) e-scooter operational data obtained through partnerships with mobility service providers such as Tier Mobility. The methodological framework is comprehensively documented with detailed technical specifications and parameter settings provided throughout the manuscript to facilitate independent replication.

Competing Interests The authors declare that they have no competing interests.

References

Abouelela M, Chaniotakis E, Antoniou C (2023). Understanding the landscape of shared-e-scooters in North America; Spatiotemporal analysis and policy insights. Transportation Research Part A, Policy and Practice, 169: 103602

Almaskati D, Kermanshachi S, Pamidimukkala A (2024). Convergence of emerging transportation trends: A comprehensive review of shared autonomous vehicles. Journal of Intelligent and Connected Vehicles, 7(3): 177–189

Bieliński T, Ważna A (2020). Electric scooter sharing and bike sharing user behaviour and characteristics. Sustainability , 12(22): 9640

Brown A (2021a). Micromobility, macro goals: Aligning scooter parking policy with broader city objectives. Transportation Research Interdisciplinary Perspectives, 12: 100508

Brown A, Klein N J, Thigpen C (2021b). Can you park your scooter there? Why scooter riders mispark and what to do about it. Findings

Brown A, Klein N J, Thigpen C, Williams N (2020). Impeding access: The frequency and characteristics of improper scooter, bike, and car parking. Transportation Research Interdisciplinary Perspectives, 4: 100099

Button K, Frye H, Reaves D (2020). Economic regulation and E-scooter networks in the USA. Research in Transportation Economics, 84: 100973

Cao Z, Zhang X, Chua K, Yu H, Zhao J (2021). E-scooter sharing to serve short-distance transit trips: A Singapore case. Transportation Research Part A, Policy and Practice, 147: 177–196

Chen J, Li K, Li K, Yu P S, Zeng Z (2021). Dynamic planning of bicycle stations in dockless public bicycle-sharing system using Gated Graph Neural Network. ACM Transactions on Intelligent Systems and Technology, 12(2): 1–22

Colovic A, Prencipe L P, Giuffrida N, Ottomanelli M (2024). A

multi-objective model to design shared e-kick scooters parking spaces in large urban areas. Journal of Transport Geography, 116: 103823

Corbane C, Pesaresi M, Kemper T, Politis P, Florczyk A J, Syrris V, Melchiorri M, Sabo F, Soille P (2019). Automated global delineation of human settlements from 40 years of Landsat satellite data archives. Big Earth Data, 3(2): 140–169

Curtale R, Liao F (2023). Travel preferences for electric sharing mobility services: Results from stated preference experiments in four European countries. Transportation Research Part C, Emerging Technologies, 155: 104321

Deveci M, Gokasar I, Pamucar D, Chen Y, Coffman D (2023). Sustainable E-scooter parking operation in urban areas using fuzzy Dombi based RAFSI model. Sustainable Cities and Society, 91: 104426

Emami E, Ramezani M (2024). Integrated operator and user-based rebalancing and recharging in dockless shared e-micromobility systems. Communications in Transportation Research, 4: 100155

Eurostat (2025). The home of high-quality statistics and data on Europe. Available at the website of ec.europa.eu/eurostat

Fazio M, Giuffrida N, Le Pira M, Inturri G, Ignaccolo M (2021). Bike oriented development: Selecting locations for cycle stations through a spatial approach. Research in Transportation Business & Management, 40: 100576

Fearnley N (2020). Micromobility – regulatory challenges and opportunities. In A. Paulsson & C. H. Sørensen (Eds.), Shaping Smart Mobility Futures: Governance and Policy Instruments in times of Sustainability Transitions. Emerald Publishing Limited. 169–186

Fuady S N, Pfaffenbichler P C, Susilo Y O (2024). Bridging the gap: Toward a holistic understanding of shared micromobility fleet development dynamics. Communications in Transportation Research, 4: 100149

Gössling S (2020). Integrating e-scooters in urban transportation: Problems, policies, and the prospect of system change. Transportation Research Part D, Transport and Environment, 79: 102230

Guo B, Li J, Zheng V W, Wang Z, Yu Z (2018). CityTransfer: Transferring inter- and intra-city knowledge for chain store site recommendation based on multi-source urban data. Proceedings of the ACM on Interactive, Mobile, Wearable and Ubiquitous Technologies, 1(4): 1–23

Guo Z, Liu J, Zhao P, Li A, Liu X (2023). Spatiotemporal heterogeneity of the shared e-scooter–public transport relationships in Stockholm and Helsinki. Transportation Research Part D, Transport and Environment, 122: 103880

Hawa L, Cui B, Sun L, El-Geneidy A (2021). Scoot over: Determinants of shared electric scooter presence in Washington D.C. Case Studies on Transport Policy, 9(2): 418–430

He S, Shin K G (2020). Dynamic flow distribution prediction for urban dockless e-scooter sharing reconfiguration. Proceedings of the Web Conference 2020, 133–143

Heumann M, Kraschewski T, Brauner T, Tilch L, Breitner M H (2021). A spatiotemporal study and location-specific trip pattern categorization of shared e-scooter usage. Sustainability (Basel), 13(22): 12527

Huang Y, Song X, Zhu Y, Zhang S, Yu J J (2023). Traffic prediction with transfer learning: A mutual information-based approach. IEEE Transactions on Intelligent Transportation Systems, 24(8): 8236–8252

Hurlet P, Manout O, Diallo A O (2024). Policy implications of shared e-scooter parking regulation: An agent-based approach. Procedia Computer Science, 238: 444–451

Khan K, Rehman S U, Aziz K, Fong S, Sarasvady S (2014). DBSCAN: Past, present and future. The Fifth International Conference on the Applications of Digital Information and Web Technologies (ICADIWT 2014), 232–238.

Klein N, Brown A, Thigpen C (2023). Clutter and compliance: Scooter parking interventions and perceptions. Active Travel Studies, 3(1): 1–16

Krauss K, Gnann T, Burgert T, Axhausen K W (2024). Faster, greener, scooter? An assessment of shared e-scooter usage based on real-world driving data. Transportation Research Part A, Policy and Practice, 181: 103997

Kuang S, Liu Y, Wang X, Wu X, Wei Y (2024). Harnessing multimodal large language models for traffic knowledge graph generation and decision-making. Communications in Transportation Research, 4: 100146

Li A, Zhao P, Liu X, Mansourian A, Axhausen K W, Qu X (2022). Comprehensive comparison of e-scooter sharing mobility: Evidence from 30 European cities. Transportation Research Part D, Transport and Environment, 105: 103229

Liu Y, Guo B, Zhang D, Zeghlache D, Chen J, Hu K, Zhang S, Zhou D, Yu Z (2021a). Knowledge transfer with weighted adversarial network for cold-start store site recommendation. ACM Transactions on Knowledge Discovery from Data, 15(3): 1–27

Liu Y, Guo B, Zhang D, Zeghlache D, Chen J, Zhang S, Zhou D, Shi X, Yu Z (2021b). MetaStore: A task-adaptative meta-learning model for optimal store placement with multi-city knowledge transfer. ACM Transactions on Intelligent Systems and Technology, 12(3): 1–23

Liu Y, Wu F, Liu Z, Wang K, Wang F, Qu X (2023). Can language models be used for real-world urban-delivery route optimization? The Innovation, 4: (6)100520

Liu Z, Shen Y, Zhu Y (2018). Inferring dockless shared bike distribution in new cities. Proceedings of the Eleventh ACM International Conference on Web Search and Data Mining, 378–386

Ma C, Xue F (2024). A review of vehicle detection methods based on computer vision. Journal of Intelligent and Connected Vehicles, 7(1): 1–18

Ma X, Cao R, Jin Y (2019). Spatiotemporal clustering analysis of bicycle sharing system with data mining approach. Information, 10(5): 163

Miller H J (2004). Tobler's First Law and Spatial Analysis. Annals of the Association of American Geographers, 94(2): 284–289

Naidu G, Zuva T, Sibanda E M (2023). A review of evaluation metrics in machine learning algorithms. In Computer science on-line conference. Cham: Springer International Publishing. 15–25

Peled I, Lee K, Jiang Y, Dauwels J, Pereira F C (2021). On the quality requirements of demand prediction for dynamic public transport. Communications in Transportation Research, 1: 100008

Pérez-Fernández O, García-Palomares J C (2021). Parking places to moped-style scooter sharing services using GIS location-allocation models and GPS data. ISPRS International Journal of Geo-Information, 10(4): 230

Raczycki K, Szymański P (2021). Transfer learning approach to

bicycle-sharing systems' station location planning using OpenStreetMap data. Proceedings of the 4th ACM SIGSPATIAL International Workshop on Advances in Resilient and Intelligent Cities, 1–12

Sandoval R, Van Geffen C, Wilbur M, Hall B, Dubey A, Barbour W, Work D B (2021). Data driven methods for effective micromobility parking. Transportation Research Interdisciplinary Perspectives, 10: 100368

Shah N R, Guo J, Han L D, Cherry C R (2023). Why do people take e-scooter trips? Insights on temporal and spatial usage patterns of detailed trip data. Transportation Research Part A, Policy and Practice, 173: 103705

Tier (2024). TIER Mobility API Documentation. Available at the website of tier-services. io

Tuli F M, Mitra S (2024). Dissecting shared e-scooters usage patterns and its impact on other transportation modes: A case study of Portland city. Travel Behaviour & Society, 36: 100812

Vinagre Díaz J J, Fernández Pozo R, Rodríguez González A B, Wilby M R, Anvari B (2024). Blind classification of e-scooter trips according to their relationship with public transport. Transportation, 51(5): 1679–1700

Wang L, Guo B, Yang Q (2018). Smart city development with urban transfer learning. Computer, 51(12): 32–41

Wang S, Miao H, Li J, Cao J (2022). Spatio-temporal knowledge transfer for urban crowd flow prediction via deep attentive adaptation networks. IEEE Transactions on Intelligent Transportation Systems, 23(5): 4695–4705

World Population Review (2025). Europe Cities by Population 2025. Available at the website of worldpopulationreview.com

Woźniak S, Szymański P (2021). Hex2vec: Context-aware embedding H3 hexagons with OpenStreetMap tags. In: Proceedings of the 4th ACM SIGSPATIAL International Workshop on AI for Geographic Knowledge Discovery, 61–71

Xiao L, Xu W (2024). Urban spatial cluster structure in metro travel networks: An explorative study of Wuhan using big and open data. Frontiers of Engineering Management, 11(2): 231–246

Xie S, Liao F (2024). Incorporating personality traits for the study of user acceptance of electric micromobility-sharing services. Transportation Research Part F: Traffic Psychology and Behaviour, 107: 1015–1030

Yan S, O'Connor N E, Liu M (2024). U-Park: A user-centric smart parking recommendation system for electric shared micromobility services. IEEE Transactions on Artificial Intelligence, 5(10): 1–15

Yang Y, Zhan J, Liu Y, Qu X (2025a). Policy-aware cross-city learning: A framework for sustainable urban governance. The Innovation, 6(9): 100986

Yang Y, Zhan J, Liu Y, Wang Q (2025b). Cross-city transfer learning: Applications and challenges for smart cities and sustainable transportation. Communications in Transportation Research, 5: 100206

Yin Z, Hardaway K, Feng Y, Kou Z, Cai H (2023). Understanding the demand predictability of bike share systems: A station-level analysis. Frontiers of Engineering Management, 10(4): 551–565

Yue J, Long Y, Wang S, Liang H (2024). Optimization of shared electric scooter deployment stations based on distance tolerance. ISPRS International Journal of Geo-Information, 13(5): 147

Yue Y, Zhuang Y, Yeh A G O, Xie J Y, Ma C L, Li Q Q (2017). Measurements of POI-based mixed use and their relationships with neighbourhood vibrancy. International Journal of Geographical Information Science, 31(4): 658–675

Zakhem M, Smith-Colin J (2021). Micromobility implementation challenges and opportunities: Analysis of e-scooter parking and high-use corridors. Transportation Research Part D, Transport and Environment, 101: 103082

Zhang F, Lv H, Xing Q, Liao F (2025). Dynamic and personalized battery-swapping recommendations for electric micro-mobility vehicles: Leveraging deep reinforcement learning. Transportation Research Part E, Logistics and Transportation Review, 201: 104268

Zhang Y, Lin D, Mi Z (2019). Electric fence planning for dockless bike-sharing services. Journal of Cleaner Production, 206: 383–393

Ziedan A, Shah N R, Brakewood C, Cherry C (2023). A method for placing shared e-scooters corrals near transit stops. SSRN Electronic Journal